Inorganic Chemistry

Communication

pubs.acs.org/IC

High Power Density of One-Compartment H_2O_2 Fuel Cells Using Pyrazine-Bridged $Fe[M^C(CN)_4]$ (M^C = Pt^{2+} and Pd^{2+}) Complexes as the Cathode

Yusuke Yamada,* Masaki Yoneda, and Shunichi Fukuzumi*

Department of Material and Life Science, Graduate School of Engineering, Osaka University, ALCA, Japan Science Technology (JST), Suita, Osaka 565-0871, Japan

Supporting Information

ABSTRACT: Pyrazine-bridged $Fe[M^C(CN)_4]$ complexes (M^C = Pt^{2+} and Pd^{2+}) with 3D porous structures were utilized as the cathode of one-compartment H_2O_2 fuel cells, which operated in 0.3 M H_2O_2, using a nickel mesh as an anode. The power density of a H_2O_2 fuel cell using pyrazine-bridged $Fe[Pt(CN)_4]$ reached 4.2 mW cm^{-2}, which is the highest value reported for the one-compartment H_2O_2 fuel cells. On the other hand, H_2O_2 fuel cells using pyrazine-bridged $M^N[Pt(CN)_4]$ (M^N = Co^{2+} and Mn^{2+}) as the cathodes exhibited power densities lower than 0.01 mW cm^{-2}, indicating that Fe^{2+} ions are indispensable to achieve the high power density.

Hydrogen peroxide (H_2O_2) has been proposed as a potential fuel in the next generation,[1−3] because H_2O_2 can be produced from O_2 abundant in air by utilizing photoenergy in the presence of a photocatalyst and an appropriate electron donor, in which acidic conditions are thermodynamically favorable.[4] The chemical energy of the produced H_2O_2 can be converted into electrical energy by using H_2O_2 fuel cells.[5−9] When a H_2O_2 fuel cell uses H_2O_2 as a fuel and O_2 as an oxidant, as is often seen in conventional fuel cells, the maximum output theoretically achievable is as low as 0.55 V, which is less than half of those of a hydrogen (H_2) fuel cell (1.23 V) and a direct methanol fuel cell (1.21 V). However, if H_2O_2 is employed not only as a fuel but also as an oxidant, the theoretical output potential increases to 1.09 V, which is somewhat smaller but comparable to those of H_2 and methanol fuel cells.[5−9] The reactions occurring at the anode and cathode of the H_2O_2 fuel cells are given by eqs 1−3.

$$\text{Anode:} \quad H_2O_2 = O_2 + 2H^+ + 2e^- \quad 0.68 \text{ V vs NHE} \tag{1}$$

$$\text{Cathode:} \quad H_2O_2 + 2H^+ + 2e^- = 2H_2O \quad 1.77 \text{ V vs NHE} \tag{2}$$

$$\text{Total:} \quad 2H_2O_2 = O_2 + 2H_2O \tag{3}$$

A benefit of the H_2O_2 fuel cell compared with H_2 and methanol fuel cells is its simple cell structure, which does not require membranes to separate the cathode and anode (Scheme 1) because electrodes for the selective reduction and oxidation of H_2O_2 can be used in one-compartment H_2O_2 fuel cells.[2,7−9]

Scheme 1. Schematic Drawing of a One-Compartment H_2O_2 Fuel Cell and an Opening Window of a Pyrazine-Bridged Cyanide Complex

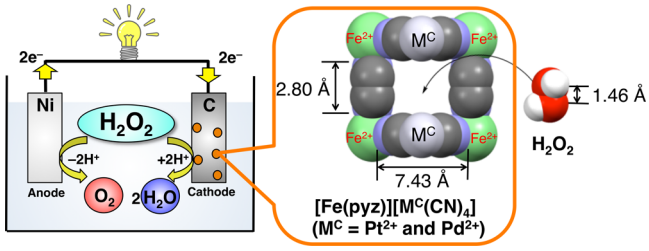

Recently, a high open-circuit potential of 0.78 V was achieved with a one-compartment H_2O_2 fuel cell operating in 0.3 M H_2O_2 at pH 1 by employing a nickel mesh and a carbon-cloth mounting $[Fe(H_2O)_2]_3[Co(CN)_6]_2$ as an anode and a cathode, respectively.[9b] A remaining challenge is increasing the power density, in which ∼1.5 mW cm^{-2} is the highest power density reported for the one-compartment H_2O_2 fuel cells so far.[8] A method to increase the power density is increasing the number of Fe^{2+} ions interacting with H_2O_2 molecules because Fe^{2+} ions coordinated by water molecules and nitrogen atoms have been reported as active species for H_2O_2 reduction at the cathode.[9b] Typically, the Fe^{2+} ions locating inside the polynuclear cyanide complexes are hardly accessible by the substrate H_2O_2 because of the small window size. The window size of homoleptic cyanide-bridged polynuclear complexes, in which the C−N bond (1.13 Å) is shorter than the O−O bond of H_2O_2 (1.46 Å), can be expanded by the combination of a polynuclear cyanide complex forming a layered structure and a bridging extraligand larger than the cyanide ligand. The 2D layers of $Fe[Pt(CN)_4]$ connected with pyrazine molecules have been reported to have porous structure with a large opening window.[10,11] The X-ray crystal structure shows that the assembly has a N···N distance of pyrazine of 2.80 Å, which is considerably longer than the C−N bond length of the cyanide ligand.[10,11] Also, pyrazine is known as a weakly bound ligand with a pK_b value of 13,[12] so that the Fe^{2+} ions are expected to interact with H_2O_2 although the pyrazine molecules coordinate to Fe^{2+} ions. We report herein the high performance of H_2O_2 fuel cells in terms of power density by using pyrazine-

Received: December 6, 2013
Published: January 17, 2014

   dx.doi.org/10.1021/ic403008d | Inorg. Chem. 2014, 53, 1272−1274

bridged $Fe[M^C(CN)_4]$ (M^C = Pt^{2+} or Pd^{2+}) complexes as cathode materials.

The pyrazine-bridged $Fe[M^C(CN)_4]$ [M^C = Pt^{2+} (**1**) and Pd^{2+} (**2**)] complexes were synthesized by the reported method with some modifications.[11] The complexes are yellow in the presence of pyrazine, although the complexes without pyrazine are white (Figure S1 in the Supporting Information, SI). The numbers of pyrazine molecules in the synthesized complexes were determined by thermogravimetry (TG) analysis under air, as shown in Figure S2a in the SI. Typically, three cascades were observed by changing the temperature from room temperature to 400 °C. The weight loss observed between room temperature and 150 °C can be assigned to the desorption of physisorbed water. The following weight loss starting from 190 until 260 °C corresponds to pyrazine desorption. The third cascade at the temperature from 300 to 360 °C is due to decomposition of the cyanide complex into corresponding metal oxides (Figure S3a in the SI). Complex **1** contained 3.0 mol of H_2O and 0.78 mol of pyrazine in each unit, as estimated from weight-loss values of the TG curve.

The microporous structure of complex **1** was confirmed by N_2 adsorption−desorption isotherm measurements (Figure S2b in the SI). The measurements performed at −196 °C revealed a type I isotherm,[13] clearly indicating the presence of micropores. The Brunauer−Emmett−Teller (BET) surface area of complex **1** was as high as 400 $m^2\ g^{-1}$. The CN stretching band of the cyanide complexes, ν(CN), as observed by IR spectroscopy, is indicative of the carbon-bound metal ion and its oxidation state.[9b,14] The CN stretching band ν(CN) of $K_2[Pt(CN)_4]$ at 2135 cm^{-1} was increasingly shifted to 2172 cm^{-1} by the replacement of K^+ ions with Fe^{2+} ions in complex **1** (Figure S4 in the SI). The higher wavenumber shift by 37 cm^{-1} agrees with the those observed in the replacement of K^+ ions to Fe^{2+} ions without ligand isomerization in polynuclear cyanide complexes.[9b,14] Complex **2** was also characterized by using the same analytical methods as those for complex **1** (Figure S3b,c in the SI). Complex **2** contains 3.7 mol of physisorbed water and 1.0 mol of pyrazine in each unit. N_2 adsorption−desorption isotherm measurements for complex **2** suggested that complex **2** has micropores with a BET surface area of 420 $m^2\ g^{-1}$. The similarity of the X-ray diffraction patterns of complexes **1** and **2** suggested that these complexes are isostructural (Figure S5 in the SI). The agreement of the main peaks with the reported diffraction peaks suggests that the structures of complexes **1** and **2** are similar to those in the literature. However, the presence of unassignable peaks indicates the partially deviated structure of complexes **1** and **2** from the reported structure.[10,11]

Complexes **1** and **2** were examined for electrochemical H_2O_2 reduction in an acetate buffer solution (pH 4), as shown in Figure S6 in the SI. In the absence of H_2O_2, each complex showed a quasi-reversible redox couple at 0.48 V vs SCE, which are assigned to the redox couple of Fe^{2+}/Fe^{3+}. The catalytic currents for H_2O_2 reduction were observed with these complexes at potentials lower than 0.4 V vs SCE in the presence of H_2O_2. The reduction peak appearing around 0 V with complex **1** (Figure S6a in the SI, red) can be assigned to H_2O_2 reduction on the Pt^{2+} ions because of the absence of the O_2 reduction peak with flowing O_2 gas (Figure S7 in the SI).

The performance of H_2O_2 fuel cells was evaluated with carbon-cloth cathodes mounting complexes **1** and **2** using a drop-casting method and a nickel mesh anode in an aqueous solution ($HClO_4$, pH 1 or 3) that contained 0.30 M H_2O_2 at room temperature (see Figure S8 in the SI for the cell performance test at pH 3). No appreciable bubble formation due to decomposition of H_2O_2 was observed on the cathode surface during the performance tests. The open-circuit potential of each H_2O_2 fuel cell operating at pH 1 was between 0.70 and 0.80 V, as shown in Figure 1a,b. The

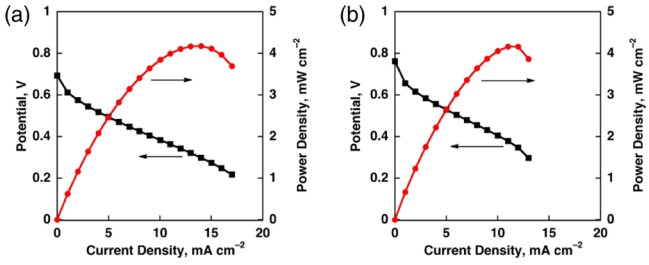

Figure 1. *I*−*V* (black) and *I*−*P* (red) curves of a one-compartment H_2O_2 fuel cell with a nickel anode and a carbon-cloth electrode modified with a pyrazine-bridged cyanide complexes pyrazine-bridged $Fe[M^C(CN)_4]$ complex [M^C = (a) Pt^{2+} (**1**) and (b) Pd^{2+} (**2**)]. Performance tests were conducted in an aqueous solution of $HClO_4$ (pH 1) that contained H_2O_2 (0.30 M) and NaCl (1.0 M). Currents and powers were normalized by the geometric surface area of an electrode.

power density of the H_2O_2 fuel cells with complexes **1** and **2** reached 4.2 mW cm^{-2}, which is more than double compared to the highest value (1.5 mW cm^{-2}) reported so far for the one-compartment H_2O_2 fuel cells.[8] The power density of a one-compartment H_2O_2 fuel cell using $[Fe(H_2O)_2][Pt(CN)_4]$ or $[Fe(H_2O)_2][Pd(CN)_4]$ was ∼2 mW cm^{-2}, which is slightly higher than the highest reported value using Prussian blue analogues (Figure S9a,b in the SI). These complexes are expected to have a 2D structure, which is advantageous to expose active ions to the substrate effectively. However, the 2D planes seem to be stacked, as evidenced by BET surface areas as small as 24 and 4 $m^2\ g^{-1}$ for $[Fe(H_2O)_2][Pt(CN)_4]$ and $[Fe(H_2O)_2][Pd(CN)_4]$, respectively (Figure S9c,d in the SI). Thus, the obtained power density was only half that with pyrazine-bridged complexes **1** and **2**. These results clearly indicate that using pyrazine as the bridging ligand improves the performance of the one-compartment H_2O_2 fuel cells in terms of power density.

The stability of a H_2O_2 fuel cell was examined by using a carbon-paste electrode, in which 25 wt % of **1** was mixed with carbon paste. Even after 25 times measurements, insignificant change was observed in the open-circuit potential and the maximum power density retained more than 80% of that for the first measurement as shown in Figure 2. However, the leached pyrazine was detected by HPLC measurements in the reaction solution after 50 times measurements where the cell performance was significantly lowered.

The importance of the Fe^{2+} ions in the pyrazine-bridged complexes was confirmed by the replacement of Fe^{2+} ions of complex **1** with Mn^{2+} and Co^{2+} ions, which have been reported as less active species for H_2O_2 reduction.[15] The power density of the H_2O_2 fuel cells using the pyrazine-bridged $Co[Pt(CN)_4]$ and $Mn[Pt(CN)_4]$ was less than 0.01 mW cm^{-2}, which is 2 orders of magnitude smaller than that using complex **1** (Figure S10 in the SI). Thus, Pt^{2+} ions are not essential to achieving the high performance of the H_2O_2 fuel cells.

In summary, pyrazine-bridged 2D polynuclear cyanide complexes containing Fe^{2+} ions, which are active species for H_2O_2 reduction, were synthesized and employed as the cathode of one-compartment H_2O_2 fuel cells. The obtained power density of the fuel cells was more than double those reported for

dx.doi.org/10.1021/ic403008d | *Inorg. Chem.* 2014, 53, 1272−1274

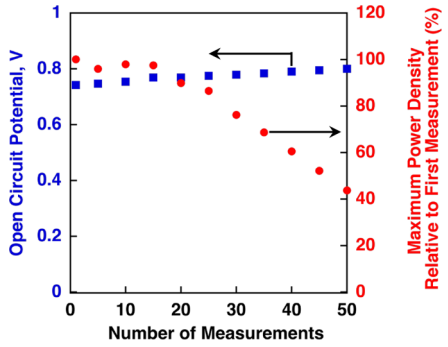

Figure 2. Changes in the open-circuit potential (■) and power density (●) after repeated measurements of a one-compartment H_2O_2 fuel cell with a nickel anode and a carbon-cloth electrode modified with a pyrazine-bridged $Fe[Pt(CN)_4]$ complex. Performance tests were conducted in an aqueous solution of $HClO_4$ (pH 1) that contained H_2O_2 (0.30 M) and NaCl (1.0 M). Currents and powers were normalized by the geometric surface area of an electrode.

one-compartment H_2O_2 fuel cells so far. The structural modification of cyanide-bridged complexes with extraligand improves the power density of the one-compartment H_2O_2 fuel cells. A remaining issue to be addressed for the one-compartment H_2O_2 fuel cells is further long-term stability of both the anode and cathode under highly acidic conditions.[9b]

■ ASSOCIATED CONTENT

Ⓢ Supporting Information

Experimental procedure, photograph and diffuse-reflectance spectrometry spectra (Figure S1), TG curves and N_2 adsorption−desorption isotherm (Figures S2 and S3), IR spectra (Figure S4), powder X-ray diffraction (Figure S5), cyclic voltammetry and cell performance (Figures S6−S10), and N_2 adsorption−desorption isotherm (Figure S9). This material is available free of charge via the Internet at http://pubs.acs.org.

■ AUTHOR INFORMATION

Corresponding Authors

*E-mail: yamada@chem.eng.osaka-u.ac.jp.
*E-mail: fukuzumi@chem.eng.osaka-u.ac.jp.

Notes

The authors declare no competing financial interest.

■ ACKNOWLEDGMENTS

This work was partially supported by Grants-in-Aid (Grants 24350069 and 25600025) from the MEXT, Japan, and NRF/MEST of Korea through the GRL program (2010-00353).

■ REFERENCES

(1) (a) Disselkamp, R. S. *Int. J. Hydrogen Energy* **2010**, *35*, 1049−1053. (b) Disselkamp, R. S. *Energy Fuels* **2008**, *22*, 2771−2774.
(2) (a) Yamada, Y.; Fukunishi, Y.; Yamazaki, S.; Fukuzumi, S. *Chem. Commun.* **2010**, *46*, 7334−7336. (b) Fukuzumi, S.; Yamada, Y.; Karlin, K. D. *Electrochim. Acta* **2012**, *82*, 493−511. (c) Fukuzumi, S.; Yamada, Y. *Aust. J. Chem.* **2014**, DOI: 10.1071/CH13436.
(3) Sanlı, A. E. *Int. J. Energy Res.* **2013**, *37*, 1488−1497.
(4) (a) Yamada, Y.; Nomura, A.; Miyahigashi, T.; Fukuzumi, S. *Chem. Commun.* **2012**, *48*, 8329−8331. (b) Yamada, Y.; Nomura, A.; Miyahigashi, T.; Ohkubo, K.; Fukuzumi, S. *J. Phys. Chem. A* **2013**, *117*, 3751−3760. (c) Yamada, Y.; Nomura, A.; Ohkubo, K.; Suenobu, T.; Fukuzumi, S. *Chem. Commun.* **2013**, *49*, 5132−5134. (d) Kato, S.; Jung, J.; Suenobu, T.; Fukuzumi, S. *Energy Environ. Sci.* **2013**, *6*, 3756−3764.
(5) Sanli, A. E.; Aytaç, A. *Int. J. Hydrogen Energy* **2011**, *36*, 869−875.
(6) (a) Yang, F.; Cheng, K.; Mo, Y.; Yu, L.; Yin, J.; Wang, G.; Cao, D. *J. Power Sources* **2012**, *217*, 562−568. (b) Yang, F.; Cheng, K.; Liu, X.; Chang, S.; Yin, J.; Du, C.; Du, L.; Wang, G.; Cao, D. *J. Power Sources* **2012**, *217*, 569−573. (c) Yang, F.; Cheng, K.; Wu, T.; Zhang, Y.; Yin, J.; Wang, G.; Cao, D. *Electrochim. Acta* **2013**, *99*, 54−61. (d) Yang, F.; Cheng, K.; Wu, T.; Zhang, Y.; Yin, J.; Wang, G.; Cao, D. *RSC Adv.* **2013**, *3*, 5483−5490.
(7) Yamazaki, S.; Siroma, Z.; Senoh, H.; Ioroi, T.; Fujiwara, N.; Yasuda, K. *J. Power Sources* **2008**, *178*, 20−25.
(8) Shaegh, S. A. M.; Nguyen, N.-T.; Ehteshami, S. M. M.; Chan, S. H. *Energy Environ. Sci.* **2012**, *5*, 8225−8228.
(9) (a) Yamada, Y.; Yoshida, S.; Honda, T.; Fukuzumi, S. *Energy Environ. Sci.* **2011**, *4*, 2822−2825. (b) Yamada, Y.; Yoneda, M.; Fukuzumi, S. *Chem.—Eur. J.* **2013**, *19*, 11733−11741.
(10) Cobo, S.; Ostrovskii, D.; Bonhommeau, S.; Vendier, L.; Molnár, G.; Salmon, L.; Tanaka, K.; Bousseksou, A. *J. Am. Chem. Soc.* **2008**, *130*, 9019−9024.
(11) Niel, V.; Martinez-Agudo, J. M.; Muñoz, M. C.; Gaspar, A. B.; Real, J. A. *Inorg. Chem.* **2001**, *40*, 3838−3839.
(12) Pettit, L. D.; Powell, K. J. *The IUPAC Stability Constants Database, SC-Database*; Academic Software: Otley, U.K., 2008.
(13) Rouquerol, F.; Rouquerol, J.; Sing, K. *Adsorption by Powder & Porous Solid*; Academic Press: London, 1999.
(14) Nakamoto, K. *Infrared and Raman Spectra of Inorganic and Coordination Compounds*, 4th ed.; Wiley Interscience: New York, 1986.
(15) Jaouen, F.; Dodelet, J.-P. *J. Phys. Chem. C* **2009**, *113*, 15422−15432.